

A High-Order Multiscale Global Atmospheric Model

Ram D. Nair

**Institute for Mathematics Applied to Geosciences (IMAGE)
Computational Information Systems Laboratory**

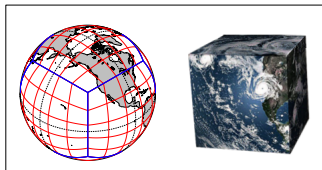
National Center for Atmospheric Research, Boulder, CO 80305

*[8th AIAA Atmospheric and Space Environments Conference,
AIAA AVIATION 2016, 15th June 2016, Washington DC.]*

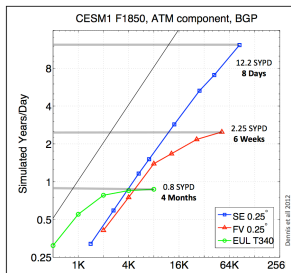


The High-Order Method Modeling Environment (HOMME)

- Horizontal Grid system (Cubed-Sphere)



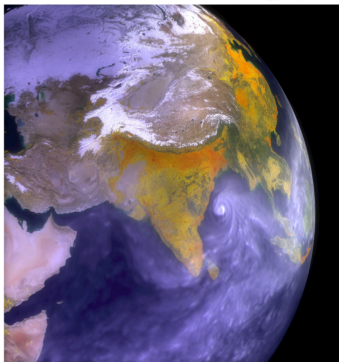
PERFORMANCE VS MODEL TYPE AT 1/4° RESOLUTION



- Developed at NCAR and DOE labs.
- HOMME hydrostatic framework is based on cubed-sphere geometry (Sadourny, 1972). Spectral Element (SE) and discontinuous Galerkin (DG) methods are used for spatial discretization
- Quasi-uniform rectangular mesh with local refinement capability, well suited for SE, DG or FV methods.
- HOMME-SE variant is used in CAM framework (CAM-SE) as a default dycore. Explit time-stepping and proven petascale capability (Dennis et al. 2012).
- HOMME currently employs pressure-based η -coordinates in the vertical with FD or VL discretization .
- Major Limitation: Hydrostatic model

Non-Hydrostatic HOMME: Why do we need this?

- Hydrostatic dynamics ($dp/dz = -\rho g$) is not suitable or valid for horizontal resolution less than 10 KM ($1/8^\circ$)
- Simulate atmospheric dynamics at ultra high-resolution (global cloud-system resolving model).
- Resolve more processes, use less parameterizations.



- Improved representation of climate variability including extreme events
- Toward exa-scale computing, more accurate climate simulation
- **Major Challenges:** Parallel efficient (local) spatial discretization. Computationally efficient time integration methods to address the acoustic modes (sound waves).

Toward a Non-Hydrostatic (NH) HOMME: Basic Design



- The NH model development in HOMME framework is named as the **High-Order Multiscale Atmospheric Model** (“HOMAM”)
- The dynamics is governed by 3D compressible Euler/Navier-Stokes system of equations, based on conservation of mass, energy, momentum etc.

- 3D Compressible Euler system (flux-form) on a rotating sphere

$$\begin{aligned} \frac{\partial \rho}{\partial t} + \nabla \cdot (\rho \mathbf{V}) &= 0 \\ \frac{\partial \rho \mathbf{V}}{\partial t} + \nabla \cdot (\rho \mathbf{V} \otimes \mathbf{V}) &= -\nabla p' - (\rho - \bar{\rho}) g \mathbf{k} \\ &\quad - 2\rho \boldsymbol{\Omega} \times \mathbf{V} + \mathbf{F}_M \\ \frac{\partial \rho \theta}{\partial t} + \nabla \cdot (\rho \theta \mathbf{V}) &= 0 \\ \frac{\partial \rho q_k}{\partial t} + \nabla \cdot (\rho q_k \mathbf{V}) &= 0 \end{aligned}$$

- $\mathbf{V} = (u, v, w)$ 3D wind field, ρ air density, p pressure, θ potential temperature, q_k moisture variables, $\boldsymbol{\Omega}$ earth's rotation rate, f Coriolis term, \mathbf{F}_M diffusive fluxes and forcing etc.
- Density $\rho = \bar{\rho} + \rho'$, and pressure $p = \bar{p} + p'$ such that the basic state follows hydrostatic balance, $\partial \bar{p} / \partial z = -\bar{\rho} g$.

Compressible Euler System in Generalized Coordinates

- The 3D compressible Euler system of equations on a rotating sphere in generalized curvilinear coordinates (x^1, x^2, x^3) can be written in tensor form (Warsi, 1992):

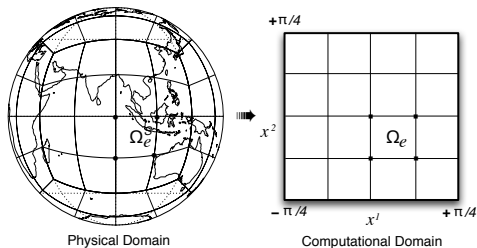
$$\begin{aligned} \frac{\partial \rho}{\partial t} + \frac{1}{\sqrt{G}} \left[\frac{\partial}{\partial x^j} (\sqrt{G} \rho u^j) \right] &= 0 \quad \{\text{Summation Implied}\} \\ \frac{\partial \rho u^i}{\partial t} + \frac{1}{\sqrt{G}} \left[\frac{\partial}{\partial x^j} [\sqrt{G} (\rho u^i u^j + p G^{ij})] \right] + \Gamma_{jk}^i (\rho u^j u^k + p G^{jk}) &= f \sqrt{G} (u^1 G^{2i} - u^2 G^{1i}) - \rho g G^{3i} \\ \frac{\partial \rho \theta}{\partial t} + \frac{1}{\sqrt{G}} \left[\frac{\partial}{\partial x^j} (\sqrt{G} \rho \theta u^j) \right] &= 0 \\ \frac{\partial \rho q}{\partial t} + \frac{1}{\sqrt{G}} \left[\frac{\partial}{\partial x^j} (\sqrt{G} \rho q u^j) \right] &= 0 \end{aligned}$$

- Where u^i is contravariant wind field, G_{ij} metric tensor, $\sqrt{G} = |G_{ij}|^{1/2}$ is the Jacobian of the transform, $G^{ij} = (G_{ij})^{-1}$, and $i, j, k \in \{1, 2, 3\}$. The associated Christoffel symbols (second kind) are defined as

$$\Gamma_{jk}^i = \frac{1}{2} G^{il} \left[\frac{\partial G_{kl}}{\partial x^j} + \frac{\partial G_{jl}}{\partial x^k} - \frac{\partial G_{kj}}{\partial x^l} \right]$$

- ρ is the air density, q is the mixing ratio (passive tracer field).

Model Equations for the Cubed-Sphere Geometry



- Equiangular central projection
- Curvilinear horizontal coordinates (x^1, x^2)
- 6 patched domains, $x^1, x^2 \in [-\pi/4, \pi/4]$
- “Cartesian-like” computational domains

- Shallow (thin) atmosphere approximation makes the the spherical domain as a vertically stacked cubed-sphere layers.
- $x^3 = \text{radius } r + \text{height } z$, s.t $z \ll r \implies (x^1, x^2, x^3) \rightarrow (x^1, x^2, z)$
- The metric tensor associated with shallow atmosphere takes a simple form,

$$G_{ij} = \begin{bmatrix} \hat{G}_{11} & \hat{G}_{12} & 0 \\ \hat{G}_{21} & \hat{G}_{22} & 0 \\ 0 & 0 & 1 \end{bmatrix}, \quad \hat{G}_{ij} = \frac{r^2}{\mu^4 \cos^2 x^1 \cos^2 x^2} \begin{bmatrix} 1 + \tan^2 x^1 & -\tan x^1 \tan x^2 \\ -\tan x^1 \tan x^2 & 1 + \tan^2 x^2 \end{bmatrix},$$

where $i, j \in \{1, 2\}$ and $\mu^2 = 1 + \tan^2 x^1 + \tan^2 x^2$. Jacobian $\sqrt{G_h} \equiv |G_{ij}|^{1/2} = |\hat{G}_{ij}|^{1/2}$

HOMAM: Vertical Grid System

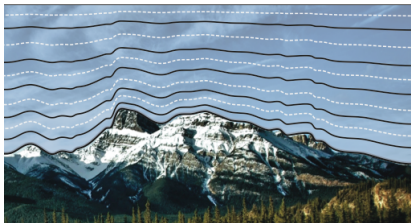


Fig Courtesy: David Hall

- Terrain-following height-based vertical z coordinate.
- Multiple options [e.g., Schär (2002), Klemp (2011), SLEVE]
- Vertical coordinate transformation (Gal-Chen & Somerville, JCP 1975), is currently adopted.

- $h_s = h_s(x^1, x^2)$ is the prescribed mountain profile and z_{top} is the top of the model domain

$$\zeta = z_{top} \frac{z - h_s}{z_{top} - h_s}, \quad z(\zeta) = h_s(x^1, x^2) + \zeta \frac{z_{top} - h_s}{z_{top}}; \quad h_s \leq z \leq z_{top}.$$

- The Jacobian associated with the transform $(x^1, x^2, z) \rightarrow (x^1, x^2, \zeta)$ is

$$\sqrt{G_v} = \left[\frac{\partial z}{\partial \zeta} \right]_{(x^1, x^2)} = 1 - \frac{h_s(x^1, x^2)}{z_{top}}$$

HOMAM: Vertical Coordinate Transform, $(x^1, x^2, z) \rightarrow (x^1, x^2, \zeta)$

- The vertical 'physical' velocity $w = dz/dt$, in (x^1, x^2, z) system
- Vertical velocity in the transformed (x^1, x^2, ζ) system is $u^3 = \tilde{w}$,

$$\tilde{w} = \frac{d\zeta}{dt}, \quad \sqrt{G_v} \tilde{w} = w + \sqrt{G_v} G_v^{13} u^1 + \sqrt{G_v} G_v^{23} u^2,$$

where (u^1, u^2) contravariant wind vectors on the cubed-sphere surface.

- Metric coefficients (*Clark 1977, JCP*)

$$\sqrt{G_v} = \left[\frac{\partial z}{\partial \zeta} \right]_{(x^1, x^2)}, \quad \sqrt{G_v} G_v^{13} \equiv \left[\frac{\partial h_s}{\partial x^1} \right]_{(z)} \left(\frac{\zeta}{z_{top}} - 1 \right), \quad \sqrt{G_v} G_v^{23} \equiv \left[\frac{\partial h_s}{\partial x^2} \right]_{(z)} \left(\frac{\zeta}{z_{top}} - 1 \right).$$

- The spacial derivatives for an arbitrary scalar ϕ can be written in terms of the transformed vertical ζ -coordinate as follows:

$$\sqrt{G_v} \frac{\partial \phi}{\partial z} = \frac{\partial \phi}{\partial \zeta}, \quad \sqrt{G_v} \frac{\partial \phi}{\partial x^i} = \frac{\partial(\sqrt{G_v} \phi)}{\partial x^i} + \frac{\partial(\sqrt{G_v} G_v^{i3} \phi)}{\partial \zeta}, \quad i = 1, 2.$$

HOMAM: 3D Transport Equation

- The transport equation in flux-form for a tracer variable q in 3D (x^1, x^2, z) coordinates can be written as

$$\frac{\partial \rho q}{\partial t} + \frac{1}{\sqrt{G_h}} \left[\frac{\partial}{\partial x^1} (\sqrt{G_h} \rho q u^1) + \frac{\partial}{\partial x^2} (\sqrt{G_h} \rho q u^2) + \frac{\partial}{\partial z} (\sqrt{G_h} \rho q w) \right] = 0$$

- Simplifications lead to logically “Cartesian-like” model equation. In computational ζ -coordinate this reduces to (2D + 1D approach)

$$\frac{\partial \psi}{\partial t} + \frac{\partial (\psi u^1)}{\partial x^1} + \frac{\partial (\psi u^2)}{\partial x^2} = - \frac{\partial (\psi \tilde{w})}{\partial \zeta},$$

where the pseudo density $\psi = \sqrt{G} \rho q$, and $\sqrt{G} = \sqrt{G_h} \sqrt{G_v}$, is the “composite” Jacobian which combines the time-independent horizontal ($\sqrt{G_h}$) and the vertical ($\sqrt{G_v}$) metric terms.

- ρq is the conservative variable and $\tilde{w} = d\zeta/dt$ is the vertical velocity due to the coordinate transformation.

HOMAM: Governing Equations in (x^1, x^2, ζ) system

- Final form of the 'perturbed' Euler system in (x^1, x^2, ζ) 3D Cubed-sphere

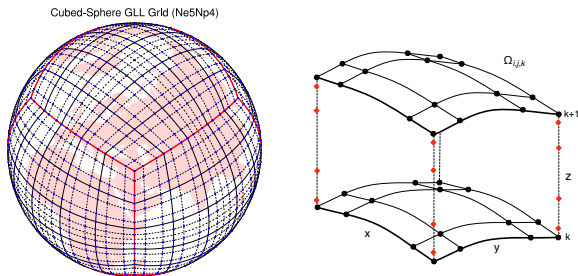
$$\frac{\partial \mathbf{U}}{\partial t} + \frac{\partial \mathbf{F}_1}{\partial x^1} + \frac{\partial \mathbf{F}_2}{\partial x^2} + \frac{\partial \mathbf{F}_3}{\partial \zeta} = \mathbf{S}(\mathbf{U}) \Rightarrow \frac{\partial \mathbf{U}}{\partial t} + \nabla \cdot \mathbf{F}(\mathbf{U}) = \mathbf{S}(\mathbf{U})$$

$$\mathbf{U} = \sqrt{G} \begin{bmatrix} \rho' \\ \rho u^1 \\ \rho u^2 \\ \rho w \\ (\rho \theta)' \end{bmatrix}, \quad \mathbf{F}_1 = \sqrt{G} \begin{bmatrix} \rho u^1 \\ \rho u^1 u^1 + p' G_h^{11} \\ \rho u^2 u^1 + p' G_h^{21} \\ \rho w u^1 \\ \rho \theta u^1 \end{bmatrix}, \quad \mathbf{F}_2 = \sqrt{G} \begin{bmatrix} \rho u^2 \\ \rho u^1 u^2 + p' G_h^{12} \\ \rho u^2 u^2 + p' G_h^{22} \\ \rho w u^2 \\ \rho \theta u^2 \end{bmatrix}$$

$$\mathbf{F}_3 = \sqrt{G} \begin{bmatrix} \rho \tilde{w} \\ \rho u^1 \tilde{w} + G_v^{13} p' \\ \rho u^2 \tilde{w} + G_v^{23} p' \\ \rho w \tilde{w} + p' / \sqrt{G_v} \\ \rho \theta \tilde{w} \end{bmatrix}, \quad \mathbf{S}(\mathbf{U}) = \sqrt{G} \begin{bmatrix} 0 \\ \sqrt{G}_h \rho f(u^1 G^{21} - u^2 G^{11}) - M_\Gamma^1 \\ \sqrt{G}_h \rho f(u^1 G^{22} - u^2 G^{12}) - M_\Gamma^2 \\ -\rho' g \\ 0 \end{bmatrix}$$

- Note: M_Γ^1, M_Γ^2 are geometric terms associated with cubed-sphere topology, they have no vertical dependence for shallow atmosphere approximation.

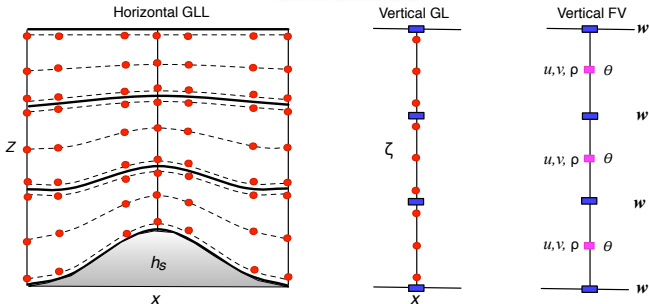
Computational Domain (Horizontal)



- **Dimensional split approach:** The computational domain \mathcal{D} is decomposed into 2D + 1D. Independent DG discretization for horizontal (x^1, x^2) cubed-sphere surfaces, and vertical (ζ) direction.
- Cubed-sphere panel is tiled with non-overlapping $N_e \times N_e$ elements, each with $N_p \times N_p$ Gauss quadrature points. This is a standard setup in HOMME framework.
- Horizontal elements are stacked in the vertical direction, which forms the 3D grid system.

Computational Domain (Vertical)

HOMAM Grid Structure



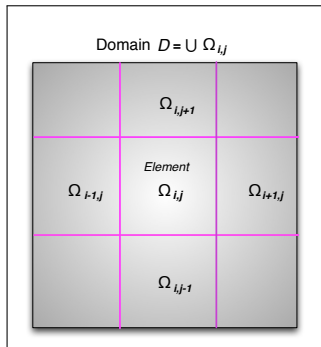
- The vertical grid line z or ζ is partitioned into V_{nel} 1D elements, each with N_g Gauss points. This is a major design change in HOMME/CAM framework.
- Currently Gauss-Legendre (GL) quadrature elements are used in the vertical, which define independent vertical levels with optimal accuracy.
- Total degrees-of-freedom (dof) is $6N_e^2 N_p^2 \times V_{nel} N_g$.
- Other possibilities: High-order FV discretization (WENO, Multi-Moment etc.)

DG Methods in 2D Cartesian Geometry

2D Scalar conservation law:

$$\frac{\partial U}{\partial t} + \nabla \cdot \mathbf{F}(U) = S(U), \quad \text{in } (0, T) \times \mathcal{D}; \quad \forall (x^1, x^2) \in \mathcal{D},$$

where $U = U(x^1, x^2, t)$, $\nabla \equiv (\partial/\partial x^1, \partial/\partial x^2)$, $\mathbf{F} = (F, G)$ is the flux function, and S is the source term.



- The domain \mathcal{D} is partitioned into non-overlapping elements Ω_{ij}
- Element edges are discontinuous
- Problem is locally solved on each element Ω_{ij}

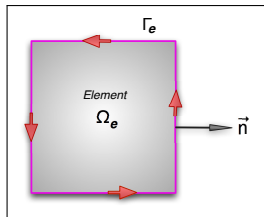
DG-2D Spatial Discretization for an Element Ω_e in \mathcal{D}

- Approximate solution U_h belongs to a vector space \mathcal{V}_h of polynomials $\mathcal{P}_N(\Omega_e)$.
- The **Galerkin formulation**: Multiplication of the basic equation by a *test function* $\varphi_h \in \mathcal{V}_h$ and integration over an element Ω_e with boundary Γ_e ,

$$\int_{\Omega_e} \left[\frac{\partial U_h}{\partial t} + \nabla \cdot \mathbf{F}(U_h) - S(U_h) \right] \varphi_h d\Omega$$

- **Weak Galerkin formulation** : Integration by parts (Green's theorem) yields:

$$\frac{\partial}{\partial t} \int_{\Omega_e} U_h \varphi_h d\Omega - \int_{\Omega_e} \mathbf{F}(U_h) \cdot \nabla \varphi_h d\Omega + \int_{\Gamma_e} \mathbf{F}(U_h) \cdot \vec{n} \varphi_h d\Gamma = \int_{\Omega_e} S(U_h) \varphi_h d\Omega$$

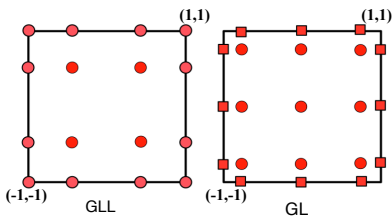
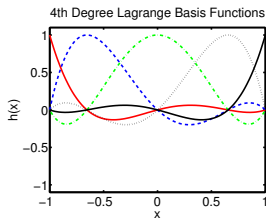


- The analytic flux $\mathbf{F}(U_h) \cdot \vec{n}$ must be replaced by a numerical flux such as the **local Lax-Friedrichs (Rusanov) Flux**:

$$\mathbf{F}(U_h) \cdot \vec{n} = \frac{1}{2} [(\mathbf{F}(U_h^-) + \mathbf{F}(U_h^+)) \cdot \vec{n} - \alpha(U_h^+ - U_h^-)]$$

- α is the upper bound on the absolute value of eigenvalues of the **flux Jacobian** $\mathbf{F}'(U)$; usually α is the local max speed of the system.

DG Method: Nodal Spatial Discretization



- Every element Ω_e is mapped onto a unique reference element $[-1, 1]^2$, with local coordinates $(\xi, \eta) \in [-1, 1]$.
Gauss-Lobatto-Legendre (GLL) or Gauss-Legendre (GL) type 2D quadrature grid.
- The nodal basis set $\{h_i(\xi) * h_j(\eta)\}$ contains tensor-product of Lagrange polynomials $h_i(\xi)$,

$$h_i(\xi)|_{GLL} = \frac{(\xi^2 - 1)P'_N(\xi)}{N(N+1)P_N(\xi_i)(\xi - \xi_i)} \quad \text{OR} \quad h_i(\xi)|_{GL} = \frac{P_{N+1}(\xi)}{P'_{N+1}(\xi_i)(\xi - \xi_i)},$$

where $P_N(\xi)$ is the N^{th} degree Legendre polynomial.

- Integrations are simplified by the quadrature rule and discrete orthogonality:

$$\int_{-1}^1 f(\xi) d\xi \approx \sum_{n=0}^N w_n f(\xi_n); \quad \int_{-1}^1 h_i(\xi) h_j(\xi) = w_i \delta_{ij},$$

where w_n are the weights associated with GLL or GL quadrature.

DG Method: Explicit Time Stepping

- The approximate solution and test functions are expressed in terms of basis function:

$$U_h(\xi, \eta) = \sum_{i=0}^N \sum_{j=0}^N U_{ij} h_i(\xi) h_j(\eta) \quad \text{for } -1 \leq \xi, \eta \leq 1$$

- Final form for the discretization leads to ODEs:

$$\frac{\partial U}{\partial t} + \nabla \cdot \mathbf{F}(U) = S(U) \quad \Rightarrow \quad \frac{d}{dt} U_h(t) = \mathcal{L}(U_h)$$

- Strong Stability Preserving third-order Runge-Kutta (SSP-RK) scheme (*Gottlieb et al., SIAM Review, 2001*)

$$\begin{aligned} U^{(1)} &= U^n + \Delta t \mathcal{L}(U^n) \\ U^{(2)} &= \frac{3}{4} U^n + \frac{1}{4} U^{(1)} + \frac{1}{4} \Delta t \mathcal{L}(U^{(1)}) \\ U^{n+1} &= \frac{1}{3} U^n + \frac{2}{3} U^{(2)} + \frac{2}{3} \Delta t \mathcal{L}(U^{(2)}). \end{aligned}$$

where the superscripts n and $n+1$ denote time levels t and $t + \Delta t$, respectively

- CFL for the DG scheme is **estimated** to be $1/(2N+1)$, where N is the degree of the polynomial (*Cockburn and Shu, 1989*).

2D NH Model: [Computational examples]

- In the transformed (x, ζ) coordinates, the Euler 2D system becomes:

$$\frac{\partial}{\partial t} \begin{bmatrix} \sqrt{G}\rho' \\ \sqrt{G}pu \\ \sqrt{G}pw \\ \sqrt{G}(\rho\theta)' \end{bmatrix} + \frac{\partial}{\partial x} \begin{bmatrix} \sqrt{G}pu \\ \sqrt{G}(\rho u^2 + p') \\ \sqrt{G}\rho uw \\ \sqrt{G}\rho u\theta \end{bmatrix} + \frac{\partial}{\partial \zeta} \begin{bmatrix} \sqrt{G}\rho\tilde{w} \\ \sqrt{G}(\rho u\tilde{w} + G^{13}p') \\ \sqrt{G}\rho w\tilde{w} + p' \\ \sqrt{G}\rho\tilde{w}\theta \end{bmatrix} = \begin{bmatrix} 0 \\ 0 \\ -\sqrt{G}\rho'g \\ 0 \end{bmatrix}.$$

- Where the metric terms (Jacobians) and new vertical velocity \tilde{w} are

$$\sqrt{G} = \frac{dz}{d\zeta}, G^{13} = \frac{d\zeta}{dx}; \quad \tilde{w} = \frac{d\zeta}{dt} = \frac{1}{\sqrt{G}}(w + \sqrt{G}G^{13}u)$$

- The metric terms are time-independent. [Bao, Kloefkorn & Nair (MWR, 2015)]
- Decompose ρ , θ and p as the sum of a **mean-state** $(\bar{\cdot})$ and **perturbation** $(\cdot)'$ such that $\rho = \bar{\rho} + \rho'$, $\theta = \bar{\theta} + \theta'$, $p = \bar{p} + p'$, $(\rho\theta) = \bar{\rho}\bar{\theta} + (\rho\theta)'$. The mean-state maintains hydrostatic balance $\frac{d\bar{p}}{d\zeta} = -\bar{\rho}g$.
- Alternative formulations are also possible [e.g., Schär (2002), Klemp (2011)] for ζ , but the system of equations remains in flux-form.

$$\frac{\partial \mathbf{U}}{\partial t} + \nabla \cdot \mathbf{F}(\mathbf{U}) = \mathbf{S}(\mathbf{U}), \quad \mathbf{U} = [\sqrt{G}\rho', \sqrt{G}pu, \sqrt{G}\rho w, \sqrt{G}(\rho\theta)']^T$$

Time Stepping Challenges for the ODE system

For the resulting ODE systems:

$$\frac{dU_h}{dt} = L(U^h), \quad t \in (0, t_T)$$

where L is the DG spatial discretization operator.

Options & Challenges

- Large aspect ratio between horizontal and vertical grid spacing imposes stringent CFL restriction ($\Delta x : \Delta z = 1 : 100$)
- Explicit time integration efficient and easy to implement.
Stringent CFL constraint \Rightarrow tiny Δt , limited practical value.

$$\frac{C\Delta t}{\bar{h}} < \frac{1}{2N+1}, \quad \bar{h} = \min\{\Delta x, \Delta z\}$$

- Implicit time integration: Unconditionally stable but generally expensive to solve for a 3D model.
- **Horizontally Explicit and Vertically Implicit (HEVI)**. Particularly useful for 3D NH modeling
- Practical approach: Split Explicit (e.g. WRF, MPAS, NICAM)

DG-NH Time Stepping with HEVI (Strang-type Split)

- Solve the ODE $d\mathbf{U}/dt = L(\mathbf{U})$ system, where $\mathbf{U} = (\sqrt{G}\rho', \sqrt{G}\rho u^1, \rho u^2, \sqrt{G}\rho w, \sqrt{G}(\rho\theta)')^T$.
- The spatial DG discretization corresponding to $L(\mathbf{U})$ is split into horizontal (H) and vertical (V) components, s.t. $L(\mathbf{U}) = L^H(\mathbf{U}) + L^V(\mathbf{U})$

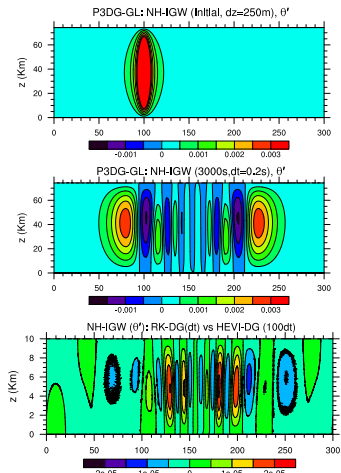
$$\begin{aligned} \mathbf{U}_1 &:= \mathbf{U}_h(t), & \frac{d}{dt}\mathbf{U}_1 &= L^H(\mathbf{U}_1) \quad \text{in } (t, t + \Delta t/2] \\ \mathbf{U}_2 &:= \mathbf{U}_1(t + \Delta t/2), & \frac{d}{dt}\mathbf{U}_2 &= L^V(\mathbf{U}_2) \quad \text{in } (t, t + \Delta t], \\ \mathbf{U}_3 &:= \mathbf{U}_2(t + \Delta t), & \frac{d}{dt}\mathbf{U}_3 &= L^H(\mathbf{U}_3) \quad \text{in } (t + \Delta t/2, t + \Delta t], \end{aligned}$$

and $\mathbf{U}_h(t + \Delta t) = \mathbf{U}_3(t + \Delta t)$.

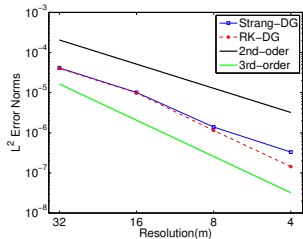
- Possible options are is to perform “ $H - V - H$ ” sequence of operations and “ $V - H - V$ ” sequence.
- The vertical part may be solved implicitly with DIRK (Diagonally Implicit Runge-Kutta; *Durran, 2010*).
- HEVI may be viewed as an IMEX Runge-Kutta (RK) method (Giraldo et al. 2009)
- For the implicit solver:
 - inner linear solver uses Jacobian-Free GMRES.
 - It usually takes 1 or 2 iterations for the outer Newton solver.

2D Inertia Gravity Wave: Convergence Study

HEVI-DG: Convergence with large aspect ratio (1 : 100)

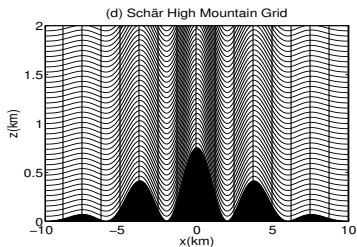


- The evolution of a potential temperature perturbation θ' (K) in a channel having periodic lateral and no-flux top/bottom boundary conditions. [Skamarock & Klemp (1994)]
- $\Delta x = 100\Delta z$, i.e., 100 times larger Δt for HEVI-DG
- Difference field θ' is $O(10^{-5})$.
- 2^{nd} -order temporal convergence.

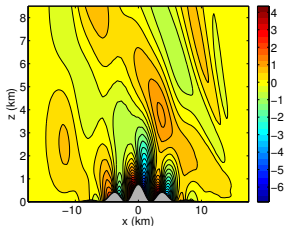


Schär High Mountain: HEVI vs Explicit

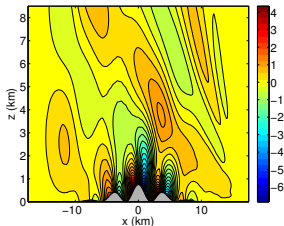
- Mountain with extreme elevation $h_0 = 750$ m (slope 55%)
- To test the robustness of HEVI as opposed to explicit RK [Bao, Kloefkorn & Nair, 2015]



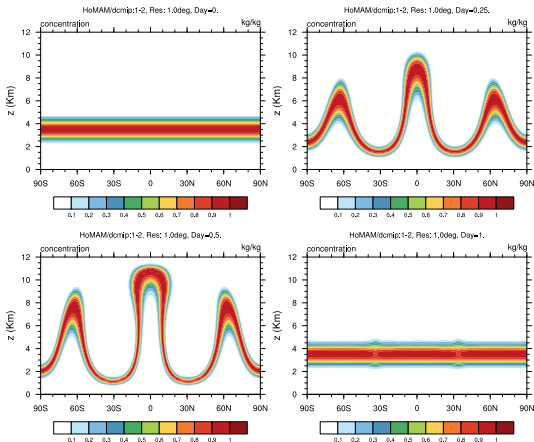
(e) HEVI: Vertical Wind w (m/s) at 1800s



(f) SSP-RK3: Vertical Wind w (m/s) at 1800s



3D Advection Test: “Hadley-like” Meridional Circulation



- HEVI, HEVE and Full (un-split) produce visually identical results.

- DCMIP: **Dynamical Core Model Intercomparison Project** (Kent et al. (2014, QJRMS))
- DCMIP-12: the flow reverses itself halfway through the simulation and returns the tracers to their initial position.
- The exact solution is known at the end of the run (1 day).
- HOMAM setup for 1° L60:
 $N_e = 30$, $N_p = 4$ (GLL);
 $V_{nel} = 15$; $N_g = 4$ (GL),
 $\Delta t = 60$ s, 1 day simulation.

3D Advection Test (DCMIP-12): Convergence Study

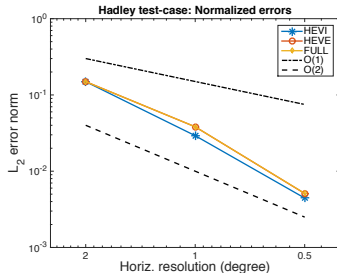
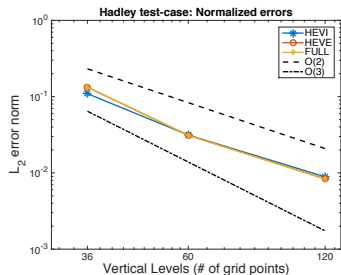


Table: Convergence Rate: DCMIP, Kent et al. (2014), Hall et al (2015) Average convergence rate for the normalized error norms for the Hadley test (DCMIP test 1-2) computed using resolutions 2° , 1° , 0.5° horizontal, and respectively with 30, 60, 120 vertical levels.

| Errors/Models: | Mcore | CAM-FV | ENDGame | CAM-SE | HOMAM |
|----------------|-------|--------|---------|--------|-------|
| l_1 | 2.22 | 1.93 | 2.18 | 2.27 | 2.62 |
| l_2 | 1.94 | 1.84 | 1.83 | 2.12 | 2.43 |
| l_∞ | 1.64 | 1.66 | 1.14 | 1.68 | 2.16 |

3D Advection: Flow Over Rough Orography (DCMIP-13)

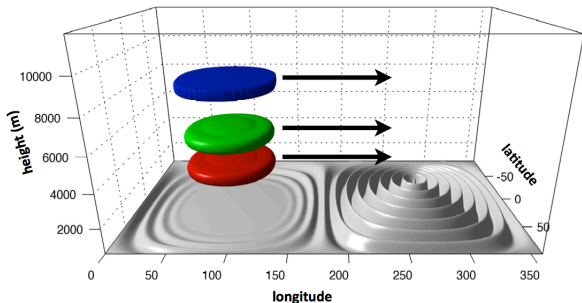
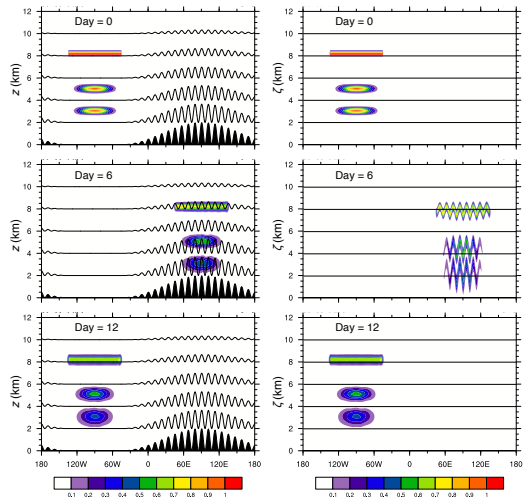


Figure: Schematic for DCMIP-13 test initial condition (Figure courtesy: David Hall)

- A series of steep concentric ring-shaped mountain ranges forms the terrain. The prescribed flow field is a constant solid-body rotation (Kent et al., 2014).
- The tracer field q is given by three thin vertically stacked cloud-like patches (non-smooth) which circumnavigate the globe and return to their initial positions after 12 days.

HOMAM: 3D Advection, Flow Over Rough Orography



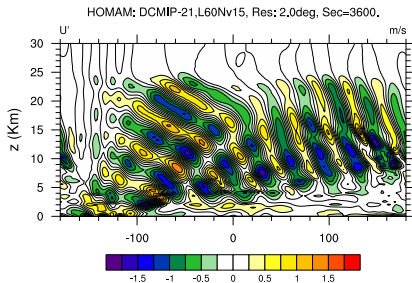
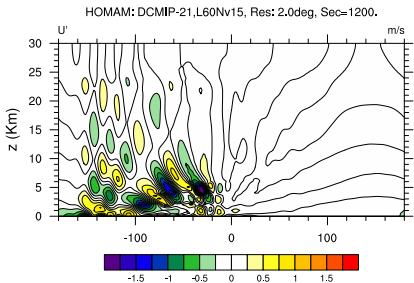
- HOMAM setup for 1° L120:
 $N_e = 30$, $N_p = 4$ (GLL);
 $V_{nel} = 30$; $N_g = 4$ (GL),
 $\Delta t = 6s$, 12 day simulation.

| Error Norm | MCore 1° L120 | CAM-SE 1° L120 | HOMAM 1° L120 |
|------------|----------------------|-----------------------|----------------------|
| l_1 | 0.83 | 0.65 | 0.78 |
| l_2 | 0.55 | 0.27 | 0.50 |
| l_∞ | 0.73 | 0.75 | 0.76 |

[Kent et al. (2014); Hall et al. (2016)]

- Vertical cross-sections along the equator for the tracer field $q = q_4$ for the DCMIP test
- The results are simulated with HOMAM using the HEVE/HEVI scheme at a horizontal resolution of 1° , 60 vertical levels, and $\Delta t = 12s$.

HOMAM: Nonhydrostatic Mountain Waves Over Rough Orography



- To study the impact of orography on an atmosphere at rest.
- DCMIP Test 2-1: NH mountain waves over a 3D Schär-type Mountain on a reduced planet, u' after 3600s
- The radius of the Earth is reduced by a factor of 500 and Coriolis effect is neglected.
- Horizontal Resolution 2° , 60 vertical levels ($N_e = 20, N_p = 4, N_g = 4$), $\Delta t = 0.20s$.
- HOMAM correctly simulates the NH mountain wave propagation.

3D Nonhydrostatic Gravity Waves: DCMIP 3-1 Test

- NH Gravity Wave test (DCMIP-31) on a reduced planet ($X = 125$), θ' after 3600s
- $N_e = 25, N_p = 4, N_g = 4$ ($\Delta x \approx \Delta z \approx 1$ km), $\Delta t = 0.25$ s
- The initial state is hydrostatically balanced and in gradient-wind balance.
- An overlaid potential temperature perturbation triggers the evolution of gravity waves.

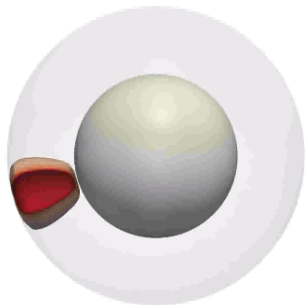
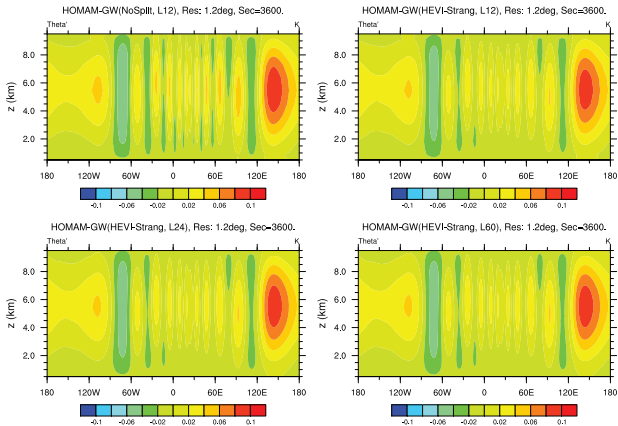


Figure: Screenshot of 3D IGW wave (Blaise et al., 2015)

DCMIP 3-1 Test: Varying the number of vertical levels

- Fix the horizontal resolution to 1 km. Vary the number of vertical levels such that $\Delta x/\Delta z = 1, 2, 5$.
- For HEVI-Strang, we use the same $\Delta t = 0.25$ s, not affected by the vertical resolution.



3D Nonhydrstatic Gravity Waves: HEVI vs Explicit

Table: Timing results of HEVI-Strang and SSP-RK3

| RK scheme | $\Delta x/\Delta z$ | Vertical Levels | Δt | Computing Time |
|-------------|---------------------|-----------------|------------|--------------------------|
| SSP-RK3 | 1 | 12 | 0.25 s | 91.0 s |
| HEVI-Strang | 1 | 12 | 0.25 s | 167.0 s (1.85) |
| SSP-RK3 | 2 | 24 | 0.125 s | 356.0 s |
| HEVI-Strang | 2 | 24 | 0.25 s | 349.0 s (0.98) |
| SSP-RK3 | 5 | 60 | 0.05 s | 2297.0 s |
| HEVI-Strang | 5 | 60 | 0.25 s | 1234.0 s (0.53) |

- HEVI maintains the parallel scalability of HOMAM

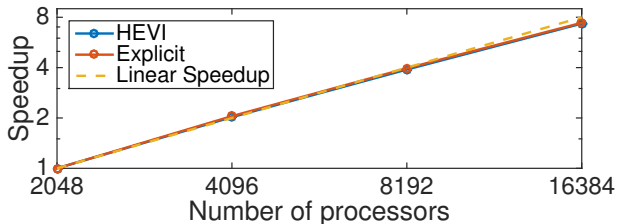


Figure: Strong Scaling

Summary

Discontinuous Galerkin Method (DGM)

- DGM with moderate order (third or fourth) is an excellent choice for atmospheric modeling, which addresses:
 - ① Local and global conservation with geometric flexibility on spherical grids. High-order accuracy and computational efficiency
 - ② Maintains the high parallel efficiency of HOMME framework
- The operator-split HEVI approach avoids stringent CFL restriction associated with vertical discretization, for NH model based on DG methods.
- The HEVI convergence shows a second-order accuracy with smooth scalar field.
- Early results with the 3D global NH model (HOMAM, split and un-split) are promising, and it performs well under benchmark test cases.

Current & Future Research:

- Extending HOMAM in CAM-SE framework and validating with DCMIP-2016 benchmark tests
- More efficient time integration schemes are desirable for practical climate simulations. Possible approaches: Multi-rate time integration in HEVI framework

Thank You!